Three-elemental models for the positive electrode of the lead/acid cell
I. Model development

R. R. Nilson
Department of Production Technology, Massey University, Private Bag, Palmerston North (New Zealand)

(Received June 17, 1992)

Abstract

Models for the discharge capacity, discharge surface area and charge surface area of a small volume of participating positive active mass in the lead/acid cell are developed. The discharge capacity model is based on equating solution and solid phase volume identities for the active mass. The discharge surface area model is a simple approximation of the likely changes in PbO_2 surface area with charge state. The charge surface area model gives actual and effective PbO_2 surface area changes with charge state, as determined from Pb^{2+} ion diffusion-controlled lobe growth within a sphere/box particle geometry. The elemental models link changes in active mass structure to distributions of current, potential and acid concentration. The models are used to study the operation of the lead/acid cell by computer simulation. They provide a new and detailed representation of the system that is valid for the wide range of operating conditions encountered during the normal working cycle of a practical lead/acid cell.

Introduction

Elemental models have been developed for the study of the lead/acid cell by simulation. Simulation provides a study approach where experimental methods are not practical. One example of this is *in situ* measurements within the finely structured active mass (AM). Simulation also provides a rapid and inexpensive tool to complement cell development by prototype testing. The validity and usefulness of simulation results depend on how well the models employed represent the real system. The elemental models are specific to the lead/acid cell and have parameters that are determined from experimental data. This specialized approach gives a close and detailed representation of the real system.

The elemental models are most powerful when used with an aggregate model. The aggregate model incorporates the effects of acid and charge transport within all solution-filled components of the cell. Together, the models simulate the discharge and charge behaviour of the lead/acid cell over a wide range of practical currents.

This paper sets out the development of each of the elemental models from concepts to mathematical formulations.

Three papers that follow give the elemental model results, the aggregate model development and the combined results [1–3].

0378-7753/93/$6.00

An elemental discharge capacity model

The discharge capacity is defined as the quantity of electrical charge that fully discharges an equivalent gram (i.e., that associated with a gram of charged PbO_2) of participating AM.

The AM structure has been characterized by pore surface area and volume distribution measurements and micrograph studies [7, 8]. These have led to the identification of two levels of structure: (i) a microstructure with fine pores providing a large reaction surface area, and (ii) a macrostructure with larger pores providing electrolyte transport passages. Both structures are thought to be needed for effective electrode operation. The micrographs have shown that the AM is arranged as a skeleton of interconnected agglomerates surrounded by macropores [4]. The agglomerates themselves are a microporous mass made up of small rock-like crystallites. The micrographs give a three-dimensional picture of the brain coral structure identified in earlier studies [9, 10].

Measurements made on partially- and fully-discharged AM showed that volume changes occurred mainly in the pores of small size (i.e., the micropores) [11]. This is consistent with a dissolution/precipitation process where $PbSO_4$ particles grow on the large surface of PbO_2 contained within the microstructure.

From the above characterization of the AM structure, the volume utilization can be simplified as follows:

- The macrostructure volume consists of solution in transport passages
- The microstructure contains all the PbO_2
- The $PbSO_4$ that results from the discharge is contained within the volume of the microstructure
- The discharge cannot proceed beyond the stage where solid $PbSO_4$ and PbO_2 fill the volume of the microstructure

Formation of $PbSO_4$ in large voids with slow discharge rates, recrystallization of $PbSO_4$ in discharged AM, and mechanical expansion of the structure during discharge [4–6] are all neglected.

By adopting this simplified representation, the local discharge capacity can be defined by the amount of electrical charge that causes the solid phase volume to fill the solution volume in the microstructure. This can be expressed as:

$$q_d = 2FV_\mu/(V_{mPbSO_4} - V_{mPbO_2}) \quad (1)$$

where q_d (A s g^{-1}) is the equivalent gram discharge capacity; F (A s mol^{-1}) is the Faraday constant; V_μ (m^3 g^{-1}) is the equivalent gram volume of solution in the charged microstructure, V_{mPbO_2} and V_{mPbSO_4} (m^3 mol^{-1}) are the molar volume of PbO_2 and $PbSO_4$, respectively.

V_μ can be determined from experimental accumulative porosity measurements after a division between the microstructure and macrostructure has been made.

An elemental discharge surface area model

The discharge surface area is defined as the surface area of PbO_2 in an equivalent gram of participating AM during discharge. It defines the area of the interface where the discharge reaction takes place.

As already described, the fully-charged structure is made up of agglomerates containing a large number of individual PbO_2 crystallites with highly angular, rock-like forms.

When the discharge begins, PbO_2 is consumed and $PbSO_4$ nuclei form randomly on the PbO_2 surface by a dissolution/precipitation process. As the discharge continues, the $PbSO_4$ particles enlarge and begin to intersect. Concurrently, the fine structure of the PbO_2 vanishes [12, 13]. Near the end of the discharge the $PbSO_4$ forms a dense structure that encloses the remaining PbO_2 [9, 11, 14].

The changes in the discharge surface area can be summarized as follows:

- Initially, fine PbO_2 structures are rapidly converted to $PbSO_4$ giving a rapid loss in PbO_2 surface area
- As the discharge continues, small PbO_2 units and angular features are consumed giving a steady loss of surface area
- Near the end of the discharge, the remaining PbO_2 particles have reduced angular features and size
- At the end of the discharge, the total surface area is made up of contributions from the PbO_2 particles and the dense $PbSO_4$ mass pressing around these particles.

These changes in the microstructure during discharge are represented schematically in Fig. 1.

The PbO_2 surface area at full charge is known from experimental measurements. At other charge states, the experimental surface area is the total of the PbO_2 and $PbSO_4$ surface areas. The PbO_2 surface area at full discharge can be taken as half the experimental surface area as a first approximation. This neglects enclosed voids and encapsulated PbO_2 within the $PbSO_4$.

For the purposes of this model, the variation of the discharge surface area between the two charge-state extremes will be taken as linear. This is an approximation for

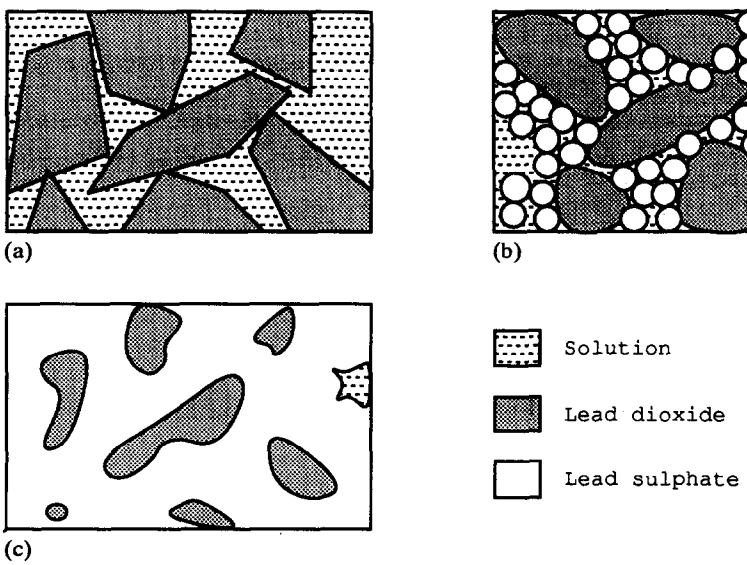

Fig. 1. Representation of the discharge process: (a) full charge: angular crystallites only; (b) partial discharge: rounded PbO_2 and $PbSO_4$ crystallites and (c) full discharge: rounded PbO_2 crystallites encapsulated in merged $PbSO_4$ crystallites.

the likely variation postulated above and gives:

$$S_{PbO_2} = X(t)(S_{cPbO_2} - S_{dPbO_2}) + -S_{dPbO_2}) + S_{dPbO_2} \quad (2)$$

where S_{PbO_2} ($m^2\ g^{-1}$) is the equivalent gram elemental discharge surface area; $X(t)$ is the charge state ($=1$ at full charge), and S_{dPbO_2} and S_{cPbO_2} ($m^2\ g^{-1}$) are the equivalent gram surface areas at full discharge and full charge, respectively.

An elemental charge surface area model

The charge surface area is defined as the PbO_2 surface area in an equivalent gram of participating AM during charge. In this case, it is not only the actual PbO_2 surface that is important but also the proportion of the actual surface where the charge reaction is taking place. The latter quantity is the effective PbO_2 surface area. At the end of the charge, the actual PbO_2 surface area is a maximum whereas the effective PbO_2 surface is zero.

Early optical microscope [9, 10] and more recent scanning electron microscopy (SEM) studies [9, 10, 12] have been made of the AM during charge. Changes in structure were attributed to a dissolution/precipitation process. At the initial stage of charge, lobes of PbO_2 developed within the encapsulating $PbSO_4$. This was taken as evidence that the PbO_2 was at all times part of an electrically conducting framework supplied with acid under the $PbSO_4$ layer. As the charge continued, PbO_2 grew on or near the $PbSO_4$ surface until the dense $PbSO_4$ structure broke down and was completely consumed. The distribution of the PbO_2 did not consistently reflect that of the $PbSO_4$ macrostructure from which it was derived. The fully charged PbO_2 was restored to agglomerates of rock-like crystallites.

Changes in the charge surface area can summarized as follows:

- The growth of PbO_2 is determined by the availability and dissolution of $PbSO_4$ and the subsequent diffusion of Pb^{2+} to the existing PbO_2 surface
- At the start of charge, featureless PbO_2 particles are enclosed in $PbSO_4$ but have electrical contact with adjacent PbO_2
- As the charge proceeds, $PbSO_4$ near the PbO_2 particles dissolves leaving a void which is filled by solution and growing PbO_2 crystallite lobes. The charge surface area increases with the growing lobes
- Initially, the $PbSO_4$ surface maintains the same shape and form but retreats fractionally from the PbO_2. Later in the charge, the $PbSO_4$ surface rapidly decreases as enclosed void volumes intersect and the dense $PbSO_4$ structure breaks down
- At the end of charge, the $PbSO_4$ is completely consumed and the PbO_2 is restored to its original form of agglomerates of rock-like crystallites

These changes in the microstructure during charge are represented schematically in Fig. 2.

What follows is a detailed model of diffusion-controlled growth of PbO_2 and is based on the factors postulated above.

A simple geometric model at full discharge

The PbO_2 at full discharge is represented by 'spheres' encapsulated in 'boxes' of $PbSO_4$. Further, each PbO_2 sphere touches four faces of the enclosing box to allow electrical contact with adjacent particles. This arrangement is illustrated in Fig. 3 where R_0 (m) is the sphere radius and half the box width; R_x (m) is half the box height, and N_x (g^{-1}) is the number of identical boxes in a gram equivalent of AM.

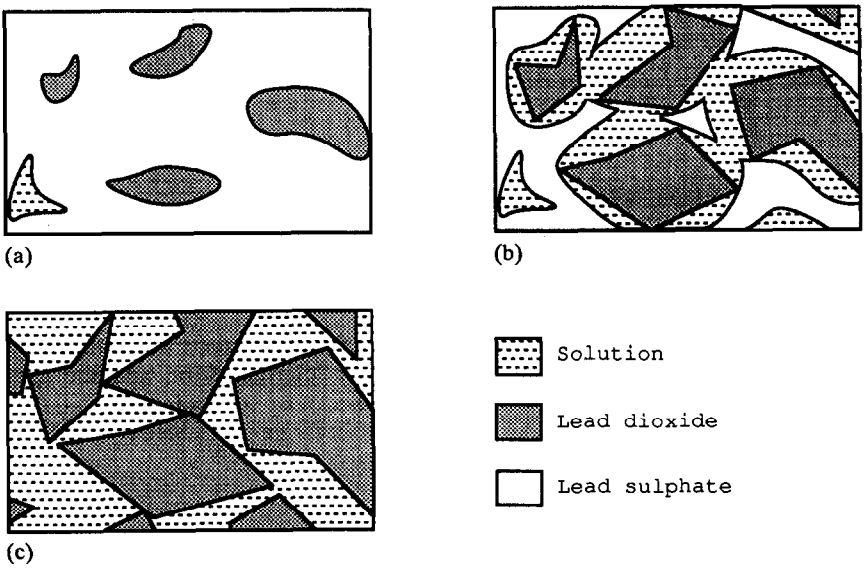

Fig. 2. Representation of the charge process: (a) full discharge: rounded PbO_2 crystallites encapsulated in $PbSO_4$; (b) partial charge: angular PbO_2 crystallites surrounded by receding $PbSO_4$, and (c) full charge: angular PhO_2 crytallites only.

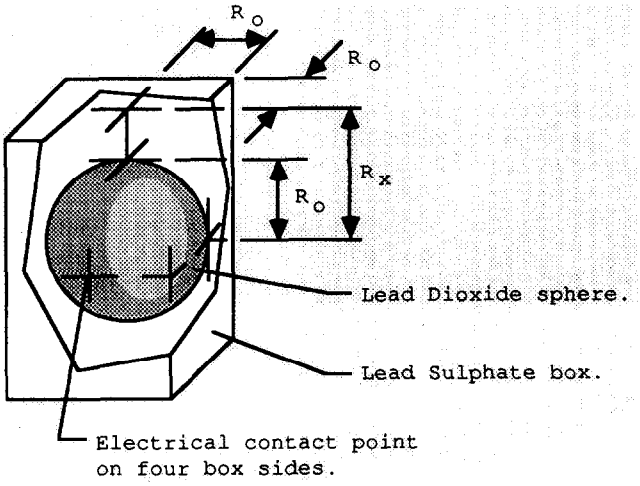

Fig. 3. Geometric model of the discharged active mass.

The values of R_0, R_x and N_x can be determined from the volume and surface area identities for the discharged AM. That is:

$$R_0 = 3f_0 V_{dPbO_2}/S_{dPbO_2} \quad (3)$$

$$N_x = 3V_{dPbO_2}/4\pi R_0^3 \quad (4)$$

$$R_x = V_{\mu Tot}/8N_x R_0^2 \quad (5)$$

where V_{dPbO_2} ($m^3\ g^{-1}$) is the equivalent gram volume of PbO_2 in the discharged AM ($1/\rho_{PbO_2} - q_d V_{mPbO_2}/2F$); $V_{\mu Tot}$ ($m^3\ g^{-1}$) is the total equivalent gram volume of the charged microstructure ($V_\mu + 1/\rho_{PbO_2}$); f_0 is the ratio of the particle surface area to that of a perfect sphere (the sphere surface factor).

$PbSO_4$ surface area formulations

The volume of $PbSO_4$ within the box, V_{xPbSO_4} (m^3), is related to the local discharge, q (A s g^{-1}), by:

$$q = 2FN_x V_{xPbSO_4}/V_{mPbSO_4} \tag{6}$$

The volume can, in turn, be used to determine the $PbSO_4$ surface area within the box, S_{xPbSO_4} (m^2), given that the surface maintains its spherical form and the fixed geometry of the box. The volume and surface area are most conveniently related by introducing the radius of the spherical surface as a common variable, R (m). This gives:

$$V_{xPbSO_4} = 8R_0^2 R_x - (4/3\pi R^3 - F_v(R)) \tag{7}$$

$$S_{xPbSO_4} = f_0(4\pi R^2 - F_s(R)) \tag{8}$$

where $F_v(R)$ (m^3) and F_s (m^2) account for the $PbSO_4$ volume and surface area loss, respectively, due to the portions of the sphere outside the boundaries of the box.

Finally, the gram equivalent $PbSO_4$ surface area, S_{PbSO_4} ($m^2\ g^{-1}$), is given by:

$$S_{PbSO_4} = N_x S_{xPbSO_4} \tag{9}$$

Actual PbO_2 surface area formulations

The supply of Pb^{2+} ions determines the precipitation volumes and, therefore, the structure of PbO_2 lobes grown on the initial PbO_2 sphere. The required surface area variation is, in turn, found from the structure of these lobes.

The volume which is supplied by Pb^{2+} ions is represented by the rectangular system shown in Fig. 4. This is a reasonable approximation to the spherical situation when the radial distance in which the reaction takes place is small, and the $PbSO_4$ surface supplying the Pb^{2+} ions is large. At the beginning of charge, this is the case because of the small distance between the $PbSO_4$ and PbO_2 surfaces. At the end of charge, this is also true since the Pb^{2+} ion concentration will rapidly fall to zero away from the $PbSO_4$ surface due to the increased demand, but reduced supply, of ions. Referring to Fig. 4, t (s) is the time from the start of charge, r (m) is the distance from a fixed point (R_0) to an arbitrary point within the supplied volume, dr (m) is the width of an elemental volume, R_0 (m) is the position of the $PbSO_4$ and PbO_2 surfaces at full discharge, $R_1(t)$ (m) is the position at which the charge reaction becomes zero, $R_2(t)$ (m) is the position of the moving $PbSO_4$ surface during charge, R_3 (m) is the position of the $PbSO_4$ surface at the end of charge, and $S_{xPbSO_4}(t)$ (m^2) is the $PbSO_4$ surface within the box during charge.

Consider next, the details of the elemental volume shown in Fig. 4. These are given in Fig. 5 where $D_{Pb^{2+}}(t)$ ($m^2\ s^{-1}$) is the diffusion coefficient for the Pb^{2+} ion in sulfuric acid solution; $j_{Pb^{2+}}(r, t)$ (mol m^{-2}) is the flux density of Pb^{2+} ions in solution; $c_{Pb^{2+}}(r, t)$ (mol m^{-3}) is the Pb^{2+} ion concentration; $n_v(t)$ is the number of growing PbO_2 lobes within the supplied volume; $r_v(r, t)$ (m) is the characteristic radius of a

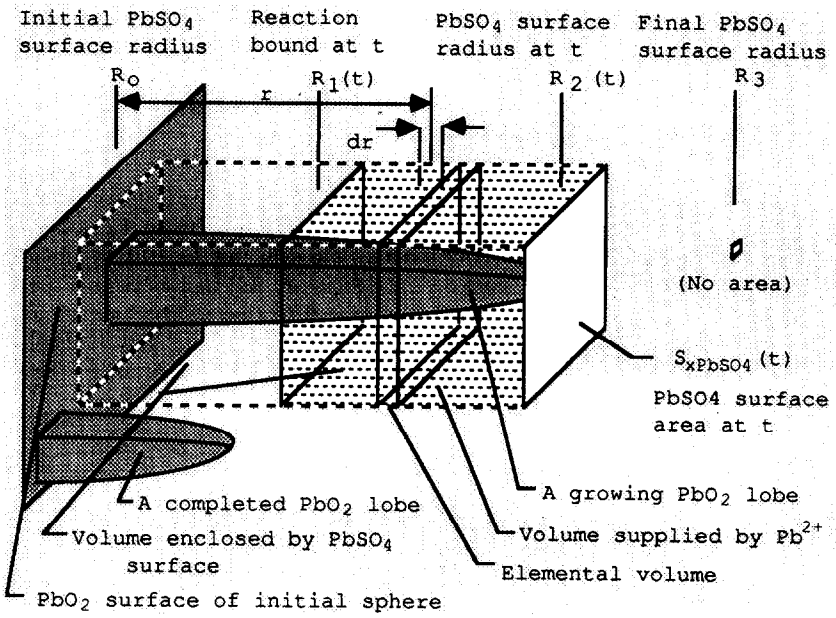

Fig. 4. Rectangular system for lead dioxide growth.

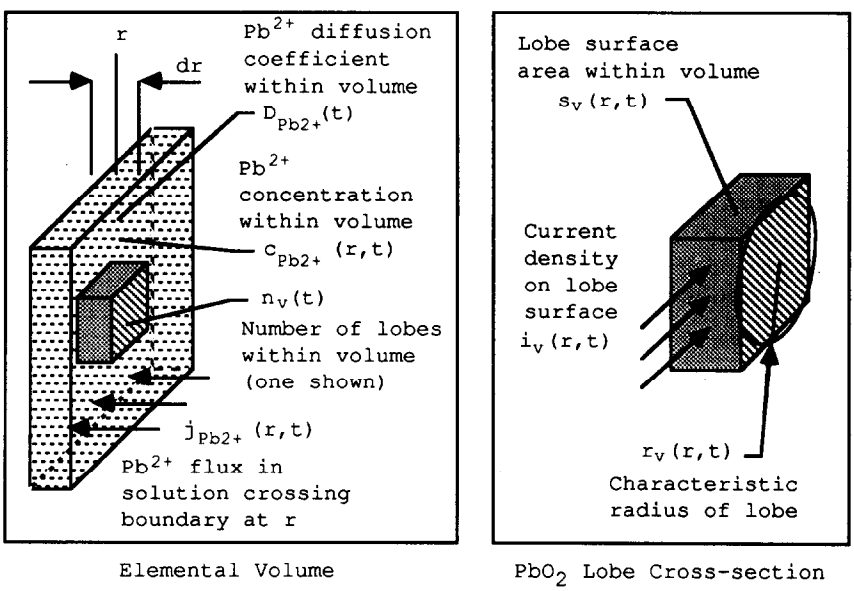

Fig. 5. Elemental volume for the Pb^{2+} ion mass balance.

lobe; $s_v(r, t)$ (m) is the lobe surface area per unit length, and $i_v(r, t)$ (A m^{-2}) is the current density on the surface of a lobe.

Writing the mass balance for Pb^{2+} ions within the solution of the elemental volume gives:

$$\frac{\delta}{\delta t}\left((S_{xPbSO_4}(t)-\pi n_v(t)r_v(r,t)^2)c_{Pb^{2+}}(r,t)\right)$$

$$=\frac{\delta}{\delta r}\left((S_{xPbSO_4}(t)-\pi n_v(t)r_v(r,t)^2)j_{Pb^{2+}}(r,t)\right)-\frac{n_v(t)s_v(r,t)i_v(r,t)}{2F} \tag{10}$$

From left to right, the terms represent accumulation, diffusion and reaction of Pb^{2+}, respectively. Migration effects are not included since potential gradients in the solution will be caused by the charge of the acid components and will not have a systematic effect on the Pb^{2+} movement. Similarly, convection effects are not included since bulk solution movement will not have a systematic effect on the direction of Pb^{2+} movement.

A more useful form for eqn. (10) is found by using equivalent or likely identities for $j_{Pb^{2+}}(r,t)$, $n_v(t)$, $s_v(r,t)$ and $i_v(r,t)$. The flux of Pb^{2+} ions can be written in terms of the concentration gradient according to Fick's first law. This gives:

$$j_{Pb^{2+}}(r,t)=-D_{Pb^{2+}}(t)\frac{\delta c_{Pb^{2+}}(r,t)}{\delta r} \tag{11}$$

The number of lobes within the volume supplied by Pb^{2+} ions can be taken as being proportional to the area that encloses that volume. That is:

$$n_v(t)=n_{v0}S_{xPbSO_4}(t)/S_{xPbSO_40} \tag{12}$$

where n_{v0} is the number of lobe sites at radius R_0, and S_{xPbSO_40} (m^2) is the $PbSO_4$ surface at radius R_0. The surface area of the lobe can be related to the characteristic radius of the lobe using a suitable geometric model. Adopting the geometric model for a conical form gives:

$$s_v(r,t)=2\pi f_v r_v(r,t)-\pi\frac{\delta r_v(r,t)^2}{\delta r} \tag{13}$$

where f_v is the surface factor for the lobe shape (the lobe surface factor, equal to unity for a circular cross section). The current density can be represented by the product of a concentration-dependent exchange current density and a potential-dependent exponential term. Taking the exchange current reaction order for Pb^{2+} as unity [15], and combining other terms into a single potential-dependent rate constant, $K_e(t)$ (A m mol^{-1}) gives:

$$i_v(r,t)=K_e(t)c_{Pb^{2+}}(r,t) \tag{14}$$

Substituting eqns. (11) to (14) into eqn. (10) gives a partial differential equation in $c_{Pb^{2+}}(r,t)$ with variable parameters $S_{xPbSO_4}(t)$ and $r_v(r,t)$. Before this can be solved for $c_{ePb^{2+}}$, boundary conditions and variation of $S_{xPbSO_4}(t)$ and $r_v(r,t)$ must be known. At the $PbSO_4$ boundary ($R_2(t)$) two conditions are known. First, the concentration at this boundary is the equilibrium concentration of Pb^{2+} ions for $PbSO_4$ in sulfuric acid solution, $c_{ePb^{2+}}(t)$ (mol m^{-3}). That is:

$$c_{Pb^{2+}}(R_2(t),t)=c_{ePb^{2+}}(t) \tag{15}$$

Second, the rate of dissolution of $PbSO_4$ is related to the concentration gradient at this boundary by Fick's first law. Assuming this, in turn, is controlled by the total current into the box, $I_x(t)$ (A), gives:

$$\frac{\delta c_{Pb^{2+}}(R_2(t),t)}{\delta r}=\frac{I_x(t)}{2FD_{Pb^{2+}}(t)S_{xPbSO_4}(t)} \tag{16}$$

At the beginning of charge, the concentration is also the equilibrium concentration. That is:

$$c_{Pb^{2+}}(r, 0) = c_{ePb^{2+}}(0) \tag{17}$$

The radius at any arbitrary point (r_1, t_1) is determined by the volume of PbO_2 deposited at r_1. This is given by the time integral of the current density and surface area product. That is:

$$r_v(r_1, t_1) = \left(\frac{V_{mPbO_2}}{2\pi F} \int_0^{t_1} i_v(r_1, t) s_v(r_1, t)\, dt \right)^{1/2} \tag{18}$$

Equation (18) needs to be qualified further by defining the maximum radius possible, as determined when an elemental volume is completely occupied by the lobes that it contains. This gives:

$$r_{vMax} = \left(\frac{b_v S_{xPbSO_40}}{\pi n_{v0}} \right)^{1/2} \tag{19}$$

where r_{vMax} (m) is the maximum radius, and b_v is the volume utilization factor (approximately unity). The initial structure is defined by:

$$r_v(0, 0) = r_{vMax} \tag{20a}$$

$$r_v(r, 0) = 0 \text{ for } r \neq 0 \tag{20b}$$

$$s_v(R_0, 0) = 4\pi f_0 R_0^2/(n_{v0}\, dr) \tag{21}$$

Solving the set of eqns. (10) to (21) gives the concentration distribution of Pb^{2+} ions. At the same time, the structure of the PbO_2 lobes, $r_v(r, t)$ and $s_v(r, t)$, is also determined. Attention can now be given to quantifying the surface area changes during charge.

The total box PbO_2 surface, $S_{xPbO_2}(t)$ (m^2), is made up of the surface area of lobes that are enclosed by the retreating $PbSO_4$ surface (growing lobes, s_{gPbO_2} (m^2)) and the surface area of lobes that have passed outside this retreating surface (completed lobes, s_{cPbO_2} (m^2)). That is:

$$S_{xPbO_2}(t) = s_{gPbO_2}(t) + s_{cPbO_2}(t) \tag{22}$$

The two terms on the right at time t_1 can be defined by:

$$s_{gPbO_2}(t_1) = \int_{R_0}^{R_2(t_1)} s_v(r, t_1)\, dr \tag{23}$$

$$s_{cPbO_2}(t_1) = \int_0^{t_1} \frac{1}{S_{xPbSO_4}(t_1)} \frac{dS_{xPbSO_4}(t)}{dt} s_{gPbO_2}(t_1)\, dt \tag{24}$$

The terms involving S_{xPbSO_4} in eqn. (24) represent the proportion of PbO_2 passing out of the growing volume in time dt.

Finally, the actual gram equivalent PbO_2 surface area, S_{PbO_2} ($m^2\ g^{-1}$), is:

$$S_{PbO_2}(t) = N_x S_{xPbO_2}(t) \tag{25}$$

Effective PbO_2 surface area formulations

The effective charge surface area is the portion of the actual surface where the electrochemical reaction rates are non-zero. That is, the surface area where the Pb^{2+} ion concentration and current density is non-zero. The formulations above show that this information is represented by parameter distributions of surface area and current density in the sphere/box model. The details of these distributions need not be retained. It is sufficient for the net current that controls the movement of mass and charge to be known. The net current can be represented by volume average parameters. In particular, the net current can be represented by an effective surface area, $S_E(t)$ ($m^2\ g^{-1}$), given an effective current density, $I_E(t)$ ($A\ m^{-2}\ g^{-1}$).

The effective surface area is defined to ensure the volume average and parameter distributions in the sphere/box model yield identical current and overpotential results for the same volume of AM (one equivalent gram).

Consider first, the equivalent gram current, $I(t)$ ($A\ g^{-1}$). This can be written as:

$$I(t) = S_E(t) I_E(t) \tag{26}$$

The current $I(t)$ must be equal to the current predicted by the sphere/box model. That is:

$$I(t) = N_x I_x(t) \tag{27}$$

where the current into a box is given by the summation of the current at the surface of growing lobes within the box. That is:

$$I_x(t) = K_e(t) \int_{R_1(t)}^{R_2(t)} s_v(r, t) c_{Pb^{2+}}(r, t)\, dr \tag{28}$$

Consider next, the overpotential at the AM surface. The overpotential for the specific structure is represented by the term $K_e(t)$ in eqn. 28. To represent the same overpotential in the volume average quantities, the effective current density can be written as:

$$I_E(t) = K_e(t) c_{ePb^{2+}}(t) \tag{29}$$

Combining eqns. (26) and (29) gives the required effective area, i.e.,

$$S_E(t) = I(t)/(K_e(t) c_{ePb^{2+}}(t)) \tag{30}$$

Elemental charge surface area model: a practical approach

The set of eqns. (10) to (30) can be solved by numerical methods. The independent variables are time, the equivalent gram current $I(t)$, the lead ion equilibrium concentration $c_{ePb^{2+}}(t)$, and the lead ion diffusion coefficient $D_{Pb^{2+}}(t)$.

The disparate time dependence of some parameters allows for two simplifications. First, since changes in structure are slow then, over a small time interval, eqn. (10) can be considered as a partial differential equation for $c_{ePb^{2+}}(r, t)$ with constant structural parameters. Second, since the independent variables are likely to change slowly compared with the transport of Pb^{2+} then, over a small time interval, the transport system can be considered to be at steady state. This means the left-hand side of eqn. (10) can

be set to zero and the partial differential equation can be replaced by an ordinary differential equation with constant parameters. The ordinary differential equation represents the situation at one point in time. The time dependence can be accommodated by updating the equation parameters for each successive time step.

The solution at one point in time is obtained by first applying the boundary conditions at $R_2(k)$ to get concentration and the concentration gradient at this point in space and, working backwards to $R_1(k)$, to define the concentration and concentration gradient at each new point in space. Unfortunately, the solution cannot be found by applying the above procedure once. This is because the value of K_e^k is not explicitly known, but rather implied, in the relationship defined by eqn. (28). Instead, an initial estimate for K_e^k must be used, the solution obtained, the current implied (form eqn. (28)) compared with the known independent variable current, K_e^k adjusted to give a more favourable comparison, and the procedure repeated until the currents agree to within acceptable limits. Having obtained the solution at one point in time, the structural parameters can be updated (from eqns. (6) to (8) and (18) given the time interval), the results extracted (eqns. (9), (22) to (25) and (30)), the time incremented, the independent variables updated, and the process repeated for the next point in time.

Performance of the elemental models

The discharge capacity model results compare well with typical cell results when the preferential discharge at the plate surface is taken into account.

The simple discharge surface area model gives a linear decrease in surface area during discharge.

The charge surface area model shows the total surface area ($PbO_2 + PbSO_4$) increases steadily during charge. This is consistent with the limited experimental data available. The model also defines the actual and effective PbO_2 surface areas for which no comparable experimental data exist.

The successful performance of the models is supported by the combined results of the elemental and aggregate models [2, 3].

Comprehensive results for the elemental models are the subject of a second paper [1].

Conclusions

Three specialized elemental models that describe changes in the positive AM structure of the lead/acid cell have been presented. The underlying reasoning and mathematical formulations for each model have been set out in detail. The models have been used in the successful computer simulation of changes in the AM structure.

The elemental models have also been used with an aggregate model to simulate the overall electrode behaviour.

References

1 R. R. Nilson and R. I. Chaplin, *J. Power Sources, 41* (1993) 13–23.
2 R. R. Nilson, *J. Power Sources, 41* (1993) 25–37.
3 R. R. Nilson and R. I. Chaplin, *J. Power Sources, 41* (1993) 39–58.

4 D. Pavlov and E. Bastavelova, *J. Electrochem. Soc., 133* (1986) 241.
5 K. Takahsahi, M. Tsubota, K. Yonezu and K. Ando, *J. Electrochem. Soc., 130* (1983) 2144.
6 I. K. Gibson and K. Peters, *J. Power Sources, 8* (1982) 143.
7 D. Pavlov and E. Bastavelova, *J. Electrochem. Soc., 131* (1984) 1468.
8 T. G. Chang, *J. Electrochem. Soc., 131* (1984) 1755.
9 A. C. Simon, C. P. Wales and S. M. Caulder, *J. Electrochem. Soc., 117* (1970) 987.
10 A. C. Simon, S. M. Caulder and J. T. Stemmle, *J. Electrochem. Soc., 122* (1975) 461.
11 P. Ekdunge and D. Simonsson, *J. Electrochem. Soc., 132* (1985) 252.
12 S. Hattori, M. Yamaura, M. Kohno, Y. Ohtani, M. Yamane and H. Nakashima, in D. H. Collins (ed.), *Power Sources 5,* Academic Press, New York, 1975, p. 139–153.
13 A. C. Simon and S. M. Caulder, in D. H. Collins (ed.), *Power Sources 5,* Academic Press, New York, 1975, pp. 109–122.
14 C. P. Wales and A. C. Simon, *J. Electrochem. Soc., 128* (1981) 2512.
15 N. A. Hampson, P. C. Jones and R. F. Phillips, *Can. J. Chem., 46* (1968) 1325.